ACS OMEGA

http://pubs.acs.org/journal/acsodf

Article

Identifying Toxicity Mechanisms Associated with Early Lanthanide Exposure through Multidimensional Genome-Wide Screening

Roger M. Pallares, Dahlia D. An, Solène Hébert, Alex Loguinov, Michael Proctor, Jonathan A. Villalobos, Kathleen A. Bjornstad, Chris J. Rosen, Chris D. Vulpe, and Rebecca J. Abergel*

Cite This: *ACS Omega* 2022, 7, 34412−34419

Read Online

ACCESS | Metrics & More | Article Recommendations | Supporting Information

ABSTRACT: Lanthanides are a series of elements essential to a wide range of applications, from clean energy production to healthcare. Despite their presence in multiple products and technologies, their toxicological characteristics have been only partly studied. Recently, our group has employed a genomic approach to extensively characterize the toxicity mechanisms of lanthanides. Even though we identified substantially different behaviors for mid and late lanthanides, the toxicological profiles of early lanthanides remained elusive. Here, we overcome this gap by describing a multidimensional genome-wide toxicogenomic study for two early lanthanides, namely, lanthanum and praseodymium. We used *Saccharomyces cerevisiae* as a model system since its genome shares many biological pathways with humans. By performing functional analysis and protein−protein interaction network analysis, we identified the main genes and proteins that participate in the yeast response to counter metal harmful effects. Moreover, our analysis also highlighted key enzymes that are dysregulated by early lanthanides, inducing cytotoxicity. Several of these genes and proteins have human orthologues, indicating that they may also participate in the human response against the metals. By highlighting the key genes and proteins in lanthanide-induced toxicity, this work may contribute to the development of new prophylactic and therapeutic strategies against lanthanide harmful exposures.

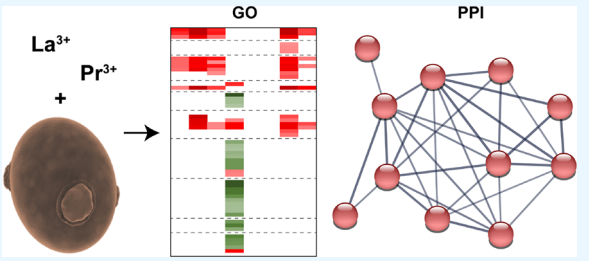

INTRODUCTION

Lanthanide metals are employed in a multitude of human-driven activities, with some essential uses in energy generation and medical diagnosis.[1,2] As a series of chemical elements, metals in the 4f block display rather similar physicochemical properties as they primarily adopt the +3 oxidation sate in aqueous solutions,[3] have similar ionic sizes (even though those decrease steadily with atomic number),[3,4] and precipitate in the form of oxides at neutral pH.[5] Although their homogeneous properties represent a challenge during their isolation, promoting renewed interest in developing more efficient separation techniques,[6−9] several key industries rely on lanthanides,[1,10] which has prompted governing agencies such as the U.S. Department of Energy to declare most of them "critical materials".[11] Among specific features of these metal ions are their characteristic narrow emission bands[12−14] that are commonly used in optoelectronics[15−17] and luminescent probes[18−22] or their magnetic properties, which motivate a rather prevalent use of gadolinium in contrast agents for magnetic resonance imaging.[23,24] Other applications may be less publicized but still pervasive, such as in the use of low concentrations of lanthanides to increase agricultural productivity, mostly in China.[25,26]

Over the past few decades, the ever-growing use of lanthanides has increased human exposure to these metals, prompting the need for a better understanding of their biological chemistry to help minimize adverse health effects. To date, the toxicological profiles of metals within the f-element series have only been partially characterized, with most published studies focusing on either their acute toxicity (by identifying median lethal doses in different models)[27−30] or their *in vivo* biodistribution after different exposures.[31−33] In addition, some studies have highlighted some key proteins that participate in lanthanide uptake and endogenous circulation.[34−36] Nevertheless, these studies did not identify the biological mechanisms disrupted by the metals that induce toxicity.

To overcome this knowledge gap, we recently started applying functional toxicogenomics to explore toxicity mechanisms associated with exposure to lanthanides. While conventional toxicogenomic methods measure variations on gene expression in cells or animal models after chemical exposure,[37,38] our approach employs *Saccharomyces cerevisiae* as a model organism as it presents many biological functions conserved in humans and its genome can be easily characterized by commercial

Received: June 28, 2022
Accepted: September 1, 2022
Published: September 16, 2022

https://doi.org/10.1021/acsomega.2c04045
ACS Omega 2022, 7, 34412−34419

methods.[39] Thus, we exploit variations on growth rates between deletion pools of yeast mutants to identify the relations between chemical exposures and genes.[40,41] Following this approach, in the past, we observed distinctive yeast cellular responses to mid and late lanthanides when deleting key genes, which provided insights into their toxicity mechanisms.[42] Nevertheless, our previous work was not sufficient to acquire mechanistic information for early lanthanides under the experimental conditions used as these metals showed low biological impact despite their known cytotoxic properties. Because our previous study screened the whole lanthanide series (except for Pm), it used one metal dose and one exposure time for each lanthanide. However, it is worth noting that the information obtained by functional toxicogenomics is dependent on the conditions employed as those can strongly affect the genes and biological paths activated after chemical exposure.[43] Hence, genome-wide studies that screen the effects of multiple parameters on the toxicogenomic profile of yeast, known as multidimensional studies, can potentially identify both condition-specific and universal biological effects that otherwise can go unnoticed.[41]

Here, we report a genome-wide toxicogenomic study that characterizes the interaction mechanisms between two early lanthanides, namely, La(III) and Pr(III), and *S. cerevisiae*. An additive effect was observed between the metal concentration and time of exposure, and only when these two parameters were above a certain value was the biological impact of the lanthanides significantly increased. Functional and protein−protein interaction (PPI) network analyses showed that the yeast response to ameliorate lanthanide toxicity relied on vesicle-mediated transport through the Golgi apparatus. Moreover, network analysis also revealed that La(III) and Pr(III) toxicity was partially caused by the disruption of key enzyme functions, particularly ATP sulfurylases. Finally, multiple genes and gene products highlighted by our analyses are conserved in humans, which suggests that they may also mediate in the interactions between early lanthanides and the human body.

METHODS

Materials. Lanthanum(III) chloride hexahydrate 99%, praseodymium(III) chloride hexahydrate 99%, magnesium(II) chloride 98%, sodium hydroxide 97%, hydrogen chloride 6 N, potassium sorbitol di-potassium hydrogen phosphate 98%, and phosphate monobasic 98% were purchased from Sigma-Aldrich (St. Louis, MO). Lanthanide solutions were prepared in 2 M HCl. Milli-Q water was obtained from the Millipore Milli-Q Integral 15 water purification system (Millipore Sigma, Burlington, MA).

Yeast Mutant Strains and Cultures. A pool of 4291 diploid yeast deletion strains (BY4743 background, Life Technologies, Carlsbad, CA) were grown in yeast extract−peptone−dextrose media (YPD, containing 1% yeast extract, 2% dextrose, and 2% peptone) with continuous 200 rpm shaking at 30 °C. Under these conditions, the doubling time (one generation) of *S. cerevisiae* is 85 min.[44]

First, to determine the required growth inhibitory concentrations (IC), wild-type yeast was grown to the mid-log phase followed by dilution down to an optical density at 600 nm (OD_{600}) of 0.0165. Different lanthanide treatments (ranging from 0.000 to 0.500 mM) were added to the yeast cells and media, and each concentration was transferred to a well in transparent 96-well plates (Grenier Bio-One, Monroe, NC). The 96-well plates containing the yeast cells were incubated with continuous 200 rpm shaking at 30 °C inside a microplate reader (Tecan Genios from Tecan Group Ltd., Männedorf, Switzerland). The OD_{600} of each well was recorded every 15 min for 24 h. The area under the growing curves were used to determine IC_5 and IC_{10} concentrations.

Screening of the Yeast Genome. The pool of deletion mutants (4291 strains) were grown for 10 or 15 generations in 700 μL of YPD media with no lanthanide (control group) and with IC_5 or IC_{10} concentrations of lanthanides at 30 °C in the microplate reader attached to an automated liquid dispensing system built in-house.[45] The 48-well plates containing the strains in YPD were continuously shaken (200 rpm), and their OD_{600} was recorded every 15 min. To avoid growth saturation and keep the strains in the log phase of growth, at every 5 generations, an inoculant of 23 μL was taken from the growth well and added by the dispensing system to a fresh well of YPD, and its respective lanthanide IC was also added to the well. The volumes were used to ensure a statistically significant representation of each deletion mutant strain. After the strains were grown for 10 or 15 generations, their growth was inhibited by transferring them to a cold plate, and then they were centrifuged to remove the supernatant, frozen down to −80 °C, and stored.

When required, the frozen yeast samples were thawed for 10 min, and the strain pool pellets were resuspended in autoclaved spheroplast buffer (4.75 g of KH_2PO_4, 2.62 g of K_2HPO_4, 109.3 g of sorbitol, and 250 μL of 1 M $MgCl_2$). Next, the strains were incubated with 1 mg/mL Zymolyase (Zymo Research, Irvine, CA) for 2 h at 37 °C in order to lyse the yeast cell walls.

The barcode DNA embedded in each strain, which identifies each strain type with a given gene deletion, was extracted with a Corbett Robotics Xtractor-Gene robot and Qiagen DX regents (Qiagen, Hilden, Germany). The quality of the extracted DNA was evaluated with a NanoQuant module (Tecan, Männedorf, Switzerland), which corroborated that the concentrations of extracted DNA ranged between 20 and 100 ng/μL and the 260/280 nm ratios were between 1.7 and 2.1.

The extracted DNA was amplified by polymerase chain reaction, where 5 μL of genomic DNA, 2 μL of primer mixtures, and 22.5 μL of Platinum SuperMix (Thermo Fisher Scientific, Waltham, MA) were combined in sealed 96-well plates. The polymerase chain reaction was programmed with the following cycles: 95 °C for 3 min; 25 cycles of 94 °C for 30 s, 55 °C for 30 s, and 72 °C for 30 s; followed by 72 °C for 10 min and holding at 10 °C. After the amplification steps were completed, the DNA was purified and concentrated with a ZR-96 DNA clean and concentrator-5 kit (Zymo Research, Irvine, CA), respectively. The resulting DNA was quantified with a Quant-iT dsDNA Assay Kit (Thermo Fisher Scientific, Waltham, MA).

The primers were removed from the purified and concentrated DNA solutions by running them in 2% agarose gels for 2 h. The DNA was then cut in a UV box and extracted with a GeneJet Gel Extraction Kit (Thermo Fisher Scientific, Waltham, MA). The resulting DNA was finally sequenced at the Vincent J. Coates Genomics Sequencing Laboratory.

It is worth noting that the results obtained by the genome-wide screening based on the automated liquid dispensing system built in-house had been previously validated via non-competitive assays.[43,46] For the validation tests, the growth of the strains with the largest $\log_2$ ratio variations was compared under competitive and non-competitive conditions.

Differential Strain Sensitivity Analysis and Functional Analysis. Differential strain sensitivity analysis (DSSA) was performed as described elsewhere.[42] Briefly, DSSA was carried

https://doi.org/10.1021/acsomega.2c04045
ACS Omega 2022, 7, 34412−34419

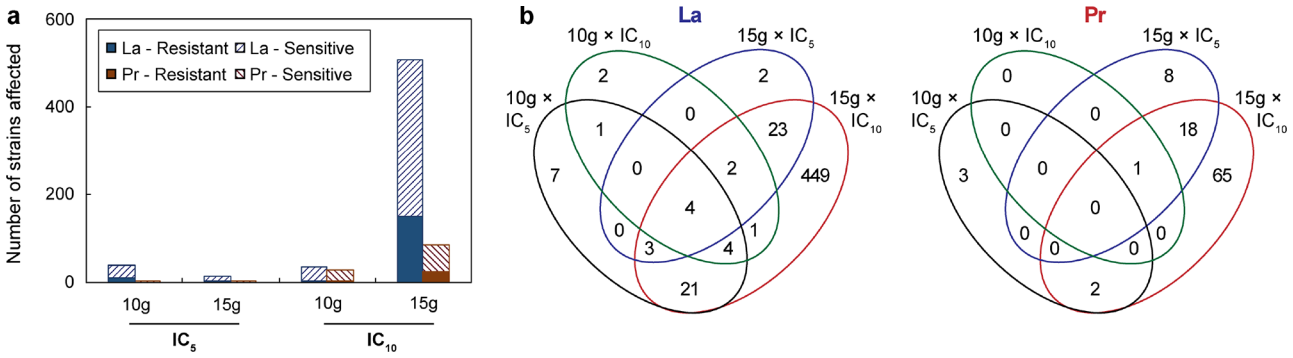

Figure 1. Resistant and sensitive strains to La(III) and Pr(III) identified by DSSA. (a) Total number of mutants determined by DSSA after being exposed to IC_5 and IC_{10} metal concentrations for 10 and 15 generations (10 and 15 g, respectively). (b) Venn diagrams of strains with disrupted growth under different experimental conditions.

out by amplifying the up and down tag barcode sequences associated to each knockout gene. Next-generation sequencing was performed with a HiSeq 2500 Sequencing System (Illumina, San Diego, CA), which was employed to count the unique barcodes associated to each mutant (gene knockout). The $\log_2$ ratio values of up and down tags were averaged, and the *p*-values were determined using Fisher's method. The barcode sequences that were significantly depleted in the treatment pools compared to the control one at a given concentration and time point ($\log_2$ ratio value < 0) identified the genes whose mutation likely led to sensitive mutants, while those barcode sequences that were significantly enriched ($\log_2$ ratio value > 0) were associated to the genes whose knockdown promoted increased mutant resistance to the treatment. A summarizing table (Dataset 1) of resistant and sensitive mutants under the different experimental conditions ($IC_5 \times 10$ g, $IC_5 \times 15$ g, $IC_{10} \times 10$ g, and $IC_{10} \times 15$ g) was obtained by establishing a cutoff of 0.05 for false discovery rate (FDR)-adjusted *p*-values.

It is worth highlighting that the mutations themselves can affect cell viability. Therefore, we evaluated the effects of each treatment (and removed the contributions of specific mutations) by comparing each strain (4291 in total) under the specific treatment to the same strain under control conditions (in the absence of lanthanide).

Gene ontology (GO) analysis of the data obtained by DSSA was performed with the David tool 6.7[47] and an FDR-adjusted *p*-value cutoff of 0.05 (Dataset S2). The FDR was employed to correct the *p*-values in order to account for multiple-hypothesis testing.[48] Protein−protein interaction network analysis was carried out by mapping the gene products of the deleted genes in the DSSA-identified mutants onto the STRING *S. cerevisiae* functional interaction network.[49] STRING provides a score (ranging between 0.00 and 1.00) for every single interaction mapped, which correlates to the likelihood of that interaction being a true positive. The analysis was performed with a score cutoff of 0.70, which was defined by the software as "high-confidence".[49] The intracellular localizations of the proteins identified in the protein−protein network analysis were screened in two databases, namely, Compartments[50] and UniProt.[51] Finally, the human orthologues of genes and gene products highlighted in our analyses were identified by screening the Alliance of Genome Resources database.[52]

RESULTS AND DISCUSSION

Differential Strain Sensitivity Analysis Identified Genes Required for Sensitivity and Tolerance to Lanthanum and Praseodymium.

The La(III) and Pr(III) concentrations that resulted in 5% (IC_5) and 10% (IC_{10}) growth inhibition of the wild-type strain were determined (Table S1) as these concentrations allow identification of specific toxicological responses to chemicals rather than overall non-specific cytotoxic effects.[40,41] Next, a pool of 4291 homozygous diploid deletion strains were grown in the presence of IC_5 or IC_{10} concentrations of La(III) or Pr(III) for 10 or 15 generations, yielding eight experimental conditions in total. These different times of exposure are commonly used in toxicogenomics because they allow determination of time-dependent responses and delayed onset effects.[40,41] Sensitive and resistant mutants to the metal treatments were identified by DSSA,[46] with their growth variations reported in the $\log_2$ scale in Dataset S1 and the total number of mutants affected under each treatment plotted (Figure 1a). The growth of only a few mutants (between 1 and 40) was disturbed at low lanthanide concentrations (IC_5) or low exposure time (10 generations). Nevertheless, under IC_{10} and 15 generations, high numbers of strains were affected, *e.g.*, 507 and 86 for La(III) and Pr(III), respectively. Hence, these results seem to suggest that the metal concentration and time of exposure have an additive effect, and only when these two parameters are above a certain value does the biological impact of the lanthanides significantly increase. Similar results were observed when comparing the percentage of resistant and sensitive strains for each treatment. The percentage of resistant mutants in comparison to the total number of disrupted strains was the highest at IC_{10} and 15 generations (30 and 28% of resistant strains for La(III) and Pr(III), respectively). In resistant strains, deleting a gene caused lower growth inhibition, suggesting that the product of the missing gene was being targeted by the metal, and when removed, the growth of the resulting mutant was less inhibited. Hence, resistant strains highlight genes and gene products that need to be studied as they may be related (directly or via secondary effects) to metal-induced toxicity. In contrast, for sensitive strains, deleting the gene caused higher growth inhibition, suggesting that the function coded by the absent gene was involved in ameliorating metal toxicity. The fact that resistant strains peaked at IC_{10} and 15 generations may indicate that at a high concentration and long exposure time, the pathways that decrease lanthanide harmful effects started to saturate, and the number of toxicity mechanisms (*i.e.*, indicated by resistant strains) associated with the metals increased. Figure 1b corroborates the additive hypothesis as the majority of strains were disrupted only at IC_{10} and 15 generations.

https://doi.org/10.1021/acsomega.2c04045
ACS Omega 2022, 7, 34412−34419

Functional Analysis Identified the Biological Functions Required for Lanthanum and Praseodymium Sensitivity and Resistance. GO enrichment analysis[53] was performed with the mutants highlighted by DSSA in order to identify enriched group of genes that share common biological characteristics (known as GO terms) for each experimental condition (Dataset S2). GO analysis allows determination of biological processes, cellular locations, and molecular functions disrupted by the chemicals studied. The majority of over-represented GO attributes (FDR-adjusted p-value < 0.01) were sensitive terms (Figure 2), and these were associated primarily

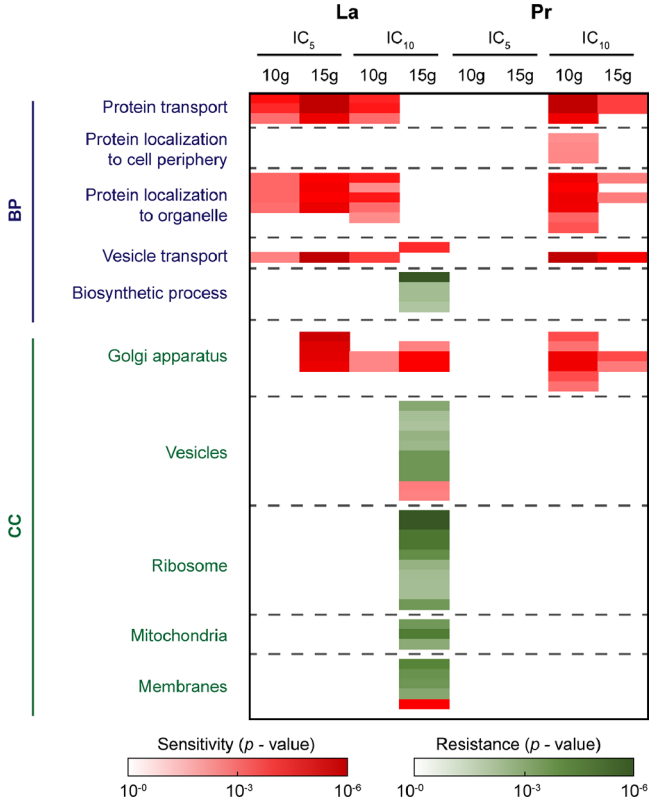

Figure 2. GO enrichment analysis of strains highlighted by DSSA. Heat map of over-represented sensitive and resistant GO terms and their corresponding FDR-adjusted p-values. The two GO domains represented in the heat map are biological process (BP), and cellular component (CC).

to protein transport and localization, vesicle-mediated transport, and the Golgi apparatus. Sensitive GO terms highlight detoxification mechanisms used by yeast to decrease metal toxicity. Hence, these results seemed to suggest that *S. cerevisiae* decreases metal toxicity by using protein- and vesicle-mediated transport to the Golgi apparatus as part of the lanthanide discharge path. These results were consistent with the known role of the Golgi apparatus as storage of biologically relevant metals and transient recipient of metals during their discharge by exocytosis.[54,55] Regarding resistant GO terms, which identify metal-inducing toxicity mechanisms, they were only observed under IC_{10} and 15 generations for La(III). These observations likely indicated that at high La(III) concentrations and long exposure times, the detoxification pathways saturated, and metal-induced toxicity started to become significant. The resistant GO terms were associated with biological processes in different organelles, including vesicles, ribosomes, and mitochondria. These results agreed with the previous literature, which reported that heavy metals disrupt the biological functions of proteins and enzymes as well as the processes that these biomolecules regulate.[56] It is worth noting that these results are substantially different from what was observed and previously reported with later lanthanides for which a similar analysis was performed: neither europium[43] nor gadolinium[46] displayed such significant metal-induced toxicity even under the greater IC_{10} exposure conditions at 15 generations.

Protein−Protein Interaction Network Analysis Highlighted the Mechanisms Responsible for Lanthanum and Praseodymium Sensitivity and Resistance. After identifying the main functional groups disrupted by La(III) and Pr(III), we carried out protein−protein interaction network analysis to discern whether the toxicological effects of the lanthanides could be associated with specific protein interactions and protein clusters. The proteins encoded by the knockdown genes in the strains highlighted by DSSA (in at least two experimental conditions) were mapped to the STRING database of *S. cerevisiae*.[49] The proteins associated with sensitive and resistant mutants were screened separately to distinguish between detoxification responses (sensitive networks) and metal-induced toxicity mechanisms (resistant networks). The sensitive networks of both metals were made of a main cluster and a few linear sub-networks (Figure 3). The two protein clusters contained COG5, COG6, and COG8, which form the conserved oligomeric Golgi (COG) complex and mediate in the fusion of vesicles to the Golgi apparatus as well as intra-Golgi trafficking.[57] Furthermore, COG7 (another component of the COG complex) was also present in the La(III) cluster. Both clusters also contained GTPase enzymes (ARL1 and/or ARL3), which in cooperation with SYS1 (another protein found in both clusters) participate in Golgi trafficking.[58,59] Furthermore, ARL1 is also a key component in the osmoregulation of potassium cations. The last protein observed in both clusters was TRS85, a component of the transport protein particle (TRAPP) complex III, which regulates endosome-to-Golgi traffic.[60] These results are consistent with our previous GO analysis (Figure 2), which highlighted functional groups associated with vesicle-mediated transport and Golgi apparatus as part of the yeast response to the lanthanides. In addition to the proteins described above, the La(III) cluster also displayed the following: VPS51, a component of the GARP protein complex, which together with the YPT6 (also found in the La(III) sensitive network) mediates in traffic from endosomes to the Golgi apparatus,[61,62] and CDC50 and DRS2, which regulate vesicle formation, including endosomes and exosomes via the trans-Golgi network.[63,64] Thus, CDC50 and DRS2 may participate in transporting the metal to the Golgi apparatus and discharging the lanthanides outside the yeast cell after Golgi processing via vesicle-mediated transport. These results are consistent with the known role of CDC50 and DRS2 in the yeast response to transition metals, such as zinc.[65]

Outside of the main clusters, both La(III) and Pr(III) networks contained SSO2 and MSO1, which participate in the vesicle fusion with membranes during exocytosis,[66,67] and VPS30, a protein that is part of the endosomal sorting complexes required for transport (ESCRT) system.[68] This protein complex participates in vesicle formation and is strongly involved in regulating calcium homeostasis.[69] Yeast using responses to regulate calcium to mitigate lanthanide toxicity is consistent with the similar coordination chemistry of these metals.[70] Moreover, lanthanides have been reported to outcompete

https://doi.org/10.1021/acsomega.2c04045
ACS Omega 2022, 7, 34412−34419

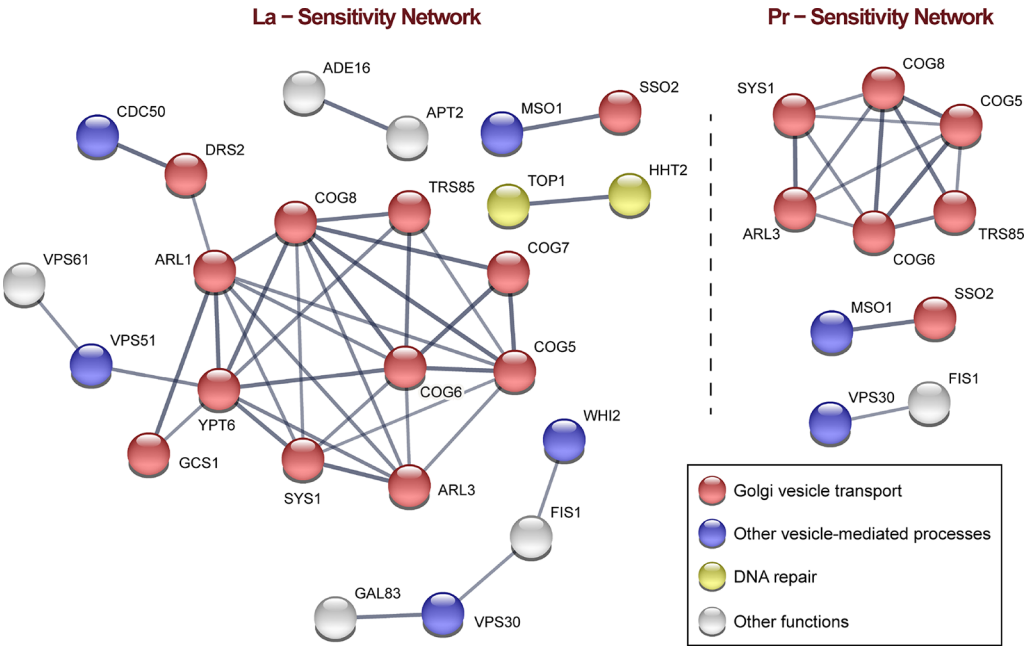

Figure 3. PPI network analysis provides insights into the mechanisms of the La(III) and Pr(III) interaction with yeast. The PPI network was built with the proteins coded by the knockdown genes of the sensitive strains. All mutants disturbed in at least two treatments were considered during the analysis. Single proteins without connections are not displayed in the figure for clarity. The PPI network analysis was performed with STRING software and a confidence cutoff of 0.70 (defined by STRING as high confidence).

calcium for protein binding sites.[36,71,72] Overall, the PPI network analysis identified 17 proteins related to vesicle-mediated transport to (or from) the Golgi apparatus as part of the yeast response to La(III) and Pr(III). These observations are consistent with the role of this organelle as storage of biologically significant cations and transient recipient of metals during their discharge from the cell.[54,55] Furthermore, several of the protein complexes identified in the analysis (ESCRT, COG, and GARP) also have an active role in the yeast response to other metals, including aluminum, cobalt, zinc, and manganese, since mutants lacking some of the proteins show higher sensitivity to the metals and can show compromised metal excretion capabilities.[73,74] In addition to proteins related to vesicle-mediated transport and Golgi apparatus, the La(III) sensitive network also contained a protein pair made by TOP1 and HHT2 (two proteins that participate in DNA replication and repair),[75,76] which likely reflects the yeast response to lanthanide-induced DNA damage.

Regarding the PPI network analysis of knockdown genes that induced yeast resistance to the metals, it only yielded a small network for La(III) (Figure S1), which was made of two protein pairs, including two ATP sulfurylases (APS1 and APS3[77,78]). Although the exact mechanism by which La(III) disrupts APS1 and APS3 functions is unknown, heavy metals are known to bind to enzymes (primarily through cysteine residues), compromise their biological activity, and cause cytotoxicity.[56]

By mapping the intracellular locations of the main proteins highlighted by PPI network analysis, we obtained an overview of the proposed yeast response to La(III) and Pr(III) (Figure 4). The main response we identified likely relies on vesicle-mediated transport of La(III) and Pr(III) to the Golgi apparatus, where the metals are stored and potentially processed before they are discharged through vesicle-mediated exocytosis. Lastly, 29 human orthologues of the genes and gene products highlighted by the network analysis were determined (Table S2), which may also play a significant role in human response against the metals through similar mechanisms to the ones identified in our study.

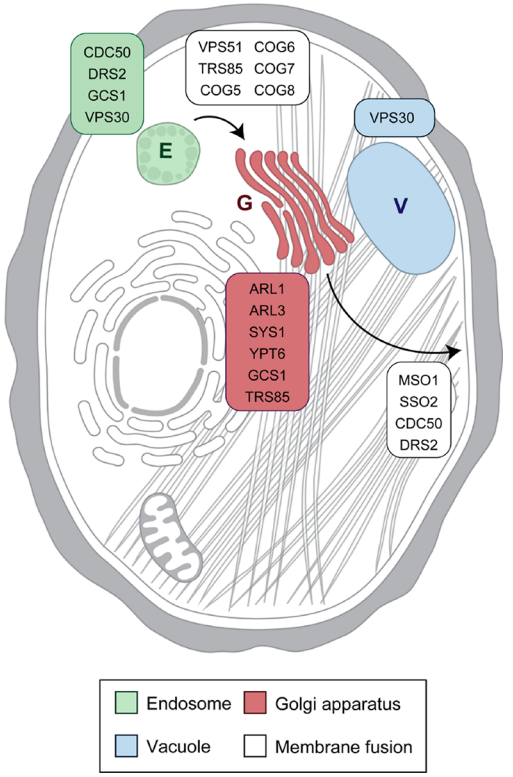

Figure 4. Intracellular yeast localizations of proteins that mediate in the yeast response to La(III) and Pr(III). E, V, and G stand for endosome, vacuole, and Golgi apparatus, respectively. The scheme was obtained with the Compartments software.[50]

https://doi.org/10.1021/acsomega.2c04045
ACS Omega 2022, 7, 34412−34419

CONCLUSIONS

In summary, we have characterized the toxicological profile of La(III) and Pr(III) in *S. cerevisiae*. The multidimensional genome-wide approach demonstrated that the metal concentration and time of exposure have an additive effect, and when both parameters are maximized, the lanthanides cause higher biological impact. GO analysis identified terms associated with vesicle-mediated transport and Golgi apparatus as the main components of the yeast response against the metal. Key protein groups (including COG, TRAPP, ESCRT, and GARP) as well as other proteins involved in membrane fusions, particularly between vesicles and Golgi apparatus, were highlighted by PPI network analysis, likely suggesting that yeast used vesicles to transport the metal to the Golgi to later be discharged through exocytosis. Moreover, PPI network analysis also identified several enzymes, such as ATP sulfurylases, that were disrupted by the metals, causing cytotoxicity. Finally, multiple proteins highlighted by PPI network analysis are conserved in humans, suggesting that those may also be involved in the interaction between early lanthanides and humans. The identification of these key gene products may contribute to the development of future prophylactic and therapeutic strategies.

ASSOCIATED CONTENT

Supporting Information

The Supporting Information is available free of charge at https://pubs.acs.org/doi/10.1021/acsomega.2c04045.

IC_5 and IC_{10} concentrations of lanthanum and praseodymium, PPI network analysis, and human orthologues of genes associated with the yeast response to lanthanum and praseodymium (PDF)

List of all pooled strains and their $\log_2$-fold growth change under different experimental conditions and list of different over-represented sensitive and resistant gene ontology terms and their FDR-adjusted *p*-values (XLSX)

AUTHOR INFORMATION

Corresponding Author

Rebecca J. Abergel − *Chemical Sciences Division, Lawrence Berkeley National Laboratory, Berkeley, California 94720, United States; Department of Nuclear Engineering, University of California, Berkeley, California 94720, United States;* orcid.org/0000-0002-3906-8761; Email: abergel@berkeley.edu

Authors

Roger M. Pallares − *Chemical Sciences Division, Lawrence Berkeley National Laboratory, Berkeley, California 94720, United States;* Present Address: Present address: Institute for Experimental Molecular Imaging (ExMI), RWTH Aachen University Hospital, Forckenbeckstr. 55, Aachen 52074, Germany (R.P.M.); orcid.org/0000-0001-7423-8706

Dahlia D. An − *Chemical Sciences Division, Lawrence Berkeley National Laboratory, Berkeley, California 94720, United States;* orcid.org/0000-0002-8763-6735

Solène Hébert − *Chemical Sciences Division, Lawrence Berkeley National Laboratory, Berkeley, California 94720, United States*

Alex Loguinov − *Center for Environmental and Human Toxicology, Department of Physiological Sciences, College of Veterinary Medicine, University of Florida, Gainesville, Florida 32611, United States*

Michael Proctor − *Center for Environmental and Human Toxicology, Department of Physiological Sciences, College of Veterinary Medicine, University of Florida, Gainesville, Florida 32611, United States*

Jonathan A. Villalobos − *Chemical Sciences Division, Lawrence Berkeley National Laboratory, Berkeley, California 94720, United States*

Kathleen A. Bjornstad − *Chemical Sciences Division, Lawrence Berkeley National Laboratory, Berkeley, California 94720, United States*

Chris J. Rosen − *Chemical Sciences Division, Lawrence Berkeley National Laboratory, Berkeley, California 94720, United States*

Chris D. Vulpe − *Center for Environmental and Human Toxicology, Department of Physiological Sciences, College of Veterinary Medicine, University of Florida, Gainesville, Florida 32611, United States;* orcid.org/0000-0001-5134-8929

Complete contact information is available at: https://pubs.acs.org/10.1021/acsomega.2c04045

Notes

The authors declare no competing financial interest.

ACKNOWLEDGMENTS

We thank Rebekah Aldrich for help with duplication of the diploid yeast deletion strains. This work was supported by the Laboratory Directed Research and Development Program at the Lawrence Berkeley National Laboratory, operating under the U.S. Department of Energy contract no. DE-AC02-05CH11231. Final analysis and assembly of the manuscript were made possible by a grant from the Berkeley Lab Foundation.

REFERENCES

(1) Kilbourn, B. T. The role of the lanthanides in the photonics, electronics and related industries. *Inorg. Chim. Acta* **1987**, *140*, 335−338.

(2) Fricker, S. P. The therapeutic application of lanthanides. *Chem. Soc. Rev.* **2006**, *35*, 524−533.

(3) Cotton, S. Introduction to the Lanthanides. In *Lanthanide and Actinide Chemistry*; John Wiley & Sons: Hoboken, NJ, 2006; pp. 1−7.

(4) Pallares, R. M.; Carter, K. P.; Faulkner, D.; Abergel, R. J. Macromolecular crystallography for f-element complex characterization. In *Methods Enzymol*; Cotruvo, J. A., Ed.; Academic Press: 2021; pp. 139−155.

(5) Diakonov, I. I.; Ragnarsdottir, K. V.; Tagirov, B. R. Standard thermodynamic properties and heat capacity equations of rare earth hydroxides: II. Ce(III)-, Pr-, Sm-, Eu(III)-, Gd-, Tb-, Dy-, Ho-, Er-, Tm-, Yb-, and Y-hydroxides. Comparison of thermochemical and solubility data. *Chem. Geol.* **1998**, *151*, 327−347.

(6) Ansari, S. A.; Mohapatra, P. K. A review on solid phase extraction of actinides and lanthanides with amide based extractants. *J. Chromatogr. A* **2017**, *1499*, 1−20.

(7) Krättli, M.; Müller-Späth, T.; Ulmer, N.; Ströhlein, G.; Morbidelli, M. Separation of Lanthanides by Continuous Chromatography. *Ind. Eng. Chem. Res.* **2013**, *52*, 8880−8886.

(8) Pallares, R. M.; Hébert, S.; Sturzbecher-Hoehne, M.; Abergel, R. J. Chelator-assisted high performance liquid chromatographic separation of trivalent lanthanides and actinides. *New J. Chem.* **2021**, *45*, 14364−14368.

(9) Pallares, R. M.; Charrier, M.; Tejedor-Sanz, S.; Li, D.; Ashby, P. D.; Ajo-Franklin, C. M.; Ralston, C. Y.; Abergel, R. J. Precision Engineering of 2D Protein Layers as Chelating Biogenic Scaffolds for Selective

Recovery of Rare-Earth Elements. *J. Am. Chem. Soc.* **2022**, *144*, 854−861.
(10) Bünzli, J.-C. G. Lanthanide Photonics: Shaping the Nanoworld. *Trends Chem.* **2019**, *1*, 751−762.
(11) DOE. *Critical Materials Strategy*; Deparment of Energy: Washignton, DC 2011.
(12) Bünzli, J.-C. G.; Comby, S.; Chauvin, A.-S.; Vandevyver, C. D. B. New Opportunities for Lanthanide Luminescence. *J. Rare Earths* **2007**, *25*, 257−274.
(13) Pallares, R. M.; Sturzbecher-Hoehne, M.; Shivaram, N. H.; Cryan, J. P.; D'Aléo, A.; Abergel, R. J. Two-Photon Antenna Sensitization of Curium: Evidencing Metal-Driven Effects on Absorption Cross Section in f-Element Complexes. *J. Phys. Chem. Lett.* **2020**, *11*, 6063−6067.
(14) Binnemans, K. Lanthanide-Based Luminescent Hybrid Materials. *Chem. Rev.* **2009**, *109*, 4283−4374.
(15) Mir, W. J.; Sheikh, T.; Arfin, H.; Xia, Z.; Nag, A. Lanthanide doping in metal halide perovskite nanocrystals: spectral shifting, quantum cutting and optoelectronic applications. *NPG Asia Mater.* **2020**, *12*, 9.
(16) Chen, X.; Sun, T.; Wang, F. Lanthanide-Based Luminescent Materials for Waveguide and Lasing. *Chem. − Asian J.* **2020**, *15*, 21−33.
(17) Pallares, R. M.; Abergel, R. J. Transforming lanthanide and actinide chemistry with nanoparticles. *Nanoscale* **2020**, *12*, 1339−1348.
(18) Abergel, R. J.; D'Aléo, A.; Ng Pak Leung, C.; Shuh, D. K.; Raymond, K. N. Using the Antenna Effect as a Spectroscopic Tool: Photophysics and Solution Thermodynamics of the Model Luminescent Hydroxypyridonate Complex [EuIII(3,4,3-LI(1,2-HOPO))]−. *Inorg. Chem.* **2009**, *48*, 10868−10870.
(19) Pallares, R. M.; An, D. D.; Tewari, P.; Wang, E. T.; Abergel, R. J. Rapid Detection of Gadolinium-Based Contrast Agents in Urine with a Chelated Europium Luminescent Probe. *ACS Sensors* **2020**, *5*, 1281−1286.
(20) Pallares, R. M.; Carter, K. P.; Zeltmann, S. E.; Tratnjek, T.; Minor, A. M.; Abergel, R. J. Selective Lanthanide Sensing with Gold Nanoparticles and Hydroxypyridinone Chelators. *Inorg. Chem.* **2020**, *59*, 2030−2036.
(21) Bui, A. T.; Roux, A.; Grichine, A.; Duperray, A.; Andraud, C.; Maury, O. Twisted Charge-Transfer Antennae for Ultra-Bright Terbium(III) and Dysprosium(III) Bioprobes. *Chem. − Eur. J.* **2018**, *24*, 3408−3412.
(22) Pallares, R. M.; Agbo, P.; Liu, X.; An, D. D.; Gauny, S. S.; Zeltmann, S. E.; Minor, A. M.; Abergel, R. J. Engineering Mesoporous Silica Nanoparticles for Targeted Alpha Therapy against Breast Cancer. *ACS Appl. Mater. Interfaces* **2020**, *12*, 40078−40084.
(23) Zhou, Z.; Lu, Z.-R. Gadolinium-based contrast agents for magnetic resonance cancer imaging. *Wiley Interdiscip. Rev.: Nanomed. Nanobiotechnol.* **2013**, *5*, 1−18.
(24) Tóth, É.; Helm, L.; Merbach, A. Relaxivity of Gadolinium(III) Complexes: Theory and Mechanism. In *The Chemistry of Contrast Agents in Medical Magnetic Resonance Imaging*; Wiley: Hoboken, NJ, 2013; pp. 25−81.
(25) Hu, Z.; Richter, H.; Sparovek, G.; Schnug, E. Physiological and Biochemical Effects of Rare Earth Elements on Plants and Their Agricultural Significance: A Review. *J. Plant Nutr.* **2004**, *27*, 183−220.
(26) Chen, W.-J.; Tao, Y.; Gu, Y.-H.; Zhao, G.-W. Effect of lanthanide chloride on photosynthesis and dry matter accumulation in tobacco seedlings. *Biol. Trace Elem. Res.* **2001**, *79*, 169−176.
(27) Haley, T. J.; Komesu, N.; Colvin, G.; Koste, L.; Upham, H. C. Pharmacology and Toxicology of Europium Chloride. *J. Pharm. Sci.* **1965**, *54*, 643−645.
(28) Tai, P.; Zhao, Q.; Su, D.; Li, P.; Stagnitti, F. Biological toxicity of lanthanide elements on algae. *Chemosphere* **2010**, *80*, 1031−1035.
(29) Gonzalez, V.; Vignati, D. A. L.; Leyval, C.; Giamberini, L. Environmental fate and ecotoxicity of lanthanides: Are they a uniform group beyond chemistry? *Environ. Int.* **2014**, *71*, 148−157.
(30) Rim, K. T.; Koo, K. H.; Park, J. S. Toxicological Evaluations of Rare Earths and Their Health Impacts to Workers: A Literature Review. *Saf. Health Work* **2013**, *4*, 12−26.
(31) Ogawa, Y.; Suzuki, S.; Naito, K.; Saito, M.; Kamata, E.; Hirose, A.; Ono, A.; Kaneko, T.; Chiba, M.; Inaba, Y.; et al. Toxicity study of europium chloride in rats. *J. Environ. Pathol., Toxicol. Oncol.* **1995**, *14*, 1−9.
(32) Bingham, D.; Dobrota, M. Distribution and excretion of lanthanides: comparison between europium salts and complexes. *BioMetals* **1994**, *7*, 142−148.
(33) Pallares, R. M.; An, D. D.; Deblonde, G. J. P.; Kullgren, B.; Gauny, S. S.; Jarvis, E. E.; Abergel, R. J. Efficient discrimination of transplutonium actinides by in vivo models. *Chem. Sci.* **2021**, *12*, 5295−5301.
(34) Tikhonova, T. N.; Shirshin, E. A.; Budylin, G. S.; Fadeev, V. V.; Petrova, G. P. Assessment of the Europium(III) Binding Sites on Albumin Using Fluorescence Spectroscopy. *J. Phys. Chem. B* **2014**, *118*, 6626−6633.
(35) Barkleit, A.; Heller, A.; Ikeda-Ohno, A.; Bernhard, G. Interaction of europium and curium with alpha-amylase. *Dalton Trans.* **2016**, *45*, 8724−8733.
(36) Pallares, R. M.; Panyala, N. R.; Sturzbecher-Hoehne, M.; Illy, M.-C.; Abergel, R. J. Characterizing the general chelating affinity of serum protein fetuin for lanthanides. *J. Biol. Inorg. Chem.* **2020**, *25*, 941−948.
(37) Pallares, R. M.; Jarvis, E.; An, D. D.; Wu, C. H.; Chang, P. Y.; Abergel, R. J. Toxicogenomic assessment of organ-specific responses following plutonium internal contamination. *Environmental Advances* **2022**, *8*, 100245.
(38) Alexander-Dann, B.; Pruteanu, L. L.; Oerton, E.; Sharma, N.; Berindan-Neagoe, I.; Módos, D.; Bender, A. Developments in toxicogenomics: understanding and predicting compound-induced toxicity from gene expression data. *Molecular Omics* **2018**, *14*, 218−236.
(39) Karathia, H.; Vilaprinyo, E.; Sorribas, A.; Alves, R. Saccharomyces cerevisiae as a Model Organism: A Comparative Study. *PLoS One* **2011**, *6*, No. e16015.
(40) Gaytán, B. D.; Loguinov, A. V.; Peñate, X.; Lerot, J.-M.; Chávez, S.; Denslow, N. D.; Vulpe, C. D. A Genome-Wide Screen Identifies Yeast Genes Required for Tolerance to Technical Toxaphene, an Organochlorinated Pesticide Mixture. *PLoS One* **2013**, *8*, No. e81253.
(41) North, M.; Tandon, V. J.; Thomas, R.; Loguinov, A.; Gerlovina, I.; Hubbard, A. E.; Zhang, L.; Smith, M. T.; Vulpe, C. D. Genome-Wide Functional Profiling Reveals Genes Required for Tolerance to Benzene Metabolites in Yeast. *PLoS One* **2011**, *6*, No. e24205.
(42) Pallares, R. M.; Faulkner, D.; An, D. D.; Hébert, S.; Loguinov, A.; Proctor, M.; Villalobos, J. A.; Bjornstad, K. A.; Rosen, C. J.; Vulpe, C.; Abergel, R. J. Genome-wide toxicogenomic study of the lanthanides sheds light on the selective toxicity mechanisms associated with critical materials. *Proc. Natl. Acad. Sci.* **2021**, *118*, No. e2025952118.
(43) Pallares, R. M.; An, D. D.; Hébert, S.; Faulkner, D.; Loguinov, A.; Proctor, M.; Villalobos, J. A.; Bjornstad, K. A.; Rosen, C. J.; Vulpe, C.; Abergel, R. J. Multidimensional genome-wide screening in yeast provides mechanistic insights into europium toxicity. *Metallomics* **2021**, *13*, mfab061.
(44) Slater, M. L.; Sharrow, S. O.; Gart, J. J. Cell cycle of Saccharomycescerevisiae in populations growing at different rates. *Proc. Natl. Acad. Sci. U. S. A.* **1977**, *74*, 3850−3854.
(45) Proctor, M.; Urbanus, M. L.; Fung, E. L.; Jaramillo, D. F.; Davis, R. W.; Nislow, C.; Giaever, G. The Automated Cell: Compound and Environment Screening System (ACCESS) for Chemogenomic Screening. In *Yeast Systems Biology: Methods and Protocols*; Castrillo, J. I.; Oliver, S. G., Eds.; Humana Press: Totowa, NJ, 2011; pp. 239−269.
(46) Pallares, R. M.; An, D. D.; Hébert, S.; Faulkner, D.; Loguinov, A.; Proctor, M.; Villalobos, J. A.; Bjornstad, K. A.; Rosen, C. J.; Vulpe, C.; Abergel, R. J. Delineating toxicity mechanisms associated with MRI contrast enhancement through a multidimensional toxicogenomic profiling of gadolinium. *Mol. Omics* **2022**, *18*, 237−248.
(47) Dennis, G., Jr.; Sherman, B. T.; Hosack, D. A.; Yang, J.; Gao, W.; Lane, H. C.; Lempicki, R. A. DAVID: Database for Annotation, Visualization, and Integrated Discovery. *Genome Biol.* **2003**, *4*, R60.
(48) Benjamini, Y.; Hochberg, Y. Controlling the False Discovery Rate: A Practical and Powerful Approach to Multiple Testing. *J. R. Stat. Soc. Series B: Stat. Methodol.* **1995**, *57*, 289−300.

https://doi.org/10.1021/acsomega.2c04045
ACS Omega 2022, 7, 34412−34419

(49) Szklarczyk, D.; Franceschini, A.; Wyder, S.; Forslund, K.; Heller, D.; Huerta-Cepas, J.; Simonovic, M.; Roth, A.; Santos, A.; Tsafou, K. P.; Kuhn, M.; Bork, P.; Jensen, L. J.; von Mering, C. STRING v10: protein−protein interaction networks, integrated over the tree of life. *Nucleic Acids Res.* **2014**, *43*, D447−D452.
(50) Binder, J. X.; Pletscher-Frankild, S.; Tsafou, K.; Stolte, C.; O'Donoghue, S. I.; Schneider, R.; Jensen, L. J. COMPARTMENTS: unification and visualization of protein subcellular localization evidence. *Database* **2014**, *2014*, DOI: 10.1093/database/bau012.
(51) The UniProt Consortium. UniProt: a hub for protein information. *Nucleic Acids Res.* **2015**, *43*, D204−D212.
(52) The Alliance of Genome Resources. Alliance of Genome Resources Portal: unified model organism research platform. *Nucleic Acids Res.* **2020**, *48*, D650−D658.
(53) Eden, E.; Navon, R.; Steinfeld, I.; Lipson, D.; Yakhini, Z. GOrilla: a tool for discovery and visualization of enriched GO terms in ranked gene lists. *BMC Bioinf.* **2009**, *10*, 48.
(54) Reddi, A. R.; Jensen, L. T.; Culotta, V. C. Manganese Homeostasis in Saccharomyces cerevisiae. *Chem. Rev.* **2009**, *109*, 4722−4732.
(55) Liu, W. Control of Calcium in Yeast Cells. In *Introduction to Modeling Biological Cellular Control Systems*; Liu, W. Ed.; Springer Milan: Milano, 2012; pp. 95−122.
(56) Wysocki, R.; Tamás, M. J. How Saccharomyces cerevisiae copes with toxic metals and metalloids. *FEMS Microbiol. Rev.* **2010**, *34*, 925−951.
(57) Whyte, J. R. C.; Munro, S. Vesicle tethering complexes in membrane traffic. *J. Cell Sci.* **2002**, *115*, 2627.
(58) Jackson, C. L. Membrane Traffic: Arl GTPases Get a GRIP on the Golgi. *Curr. Biol.* **2003**, *13*, R174−R176.
(59) Setty, S. R. G.; Strochlic, T. I.; Tong, A. H. Y.; Boone, C.; Burd, C. G. Golgi targeting of ARF-like GTPase Arl3p requires its Nα-acetylation and the integral membrane protein Sys1p. *Nat. Cell Biol.* **2004**, *6*, 414−419.
(60) Thomas, L. L.; Joiner, A. M. N.; Fromme, J. C. The TRAPPIII complex activates the GTPase Ypt1 (Rab1) in the secretory pathway. *J. Cell Biol.* **2018**, *217*, 283−298.
(61) Eising, S.; Thiele, L.; Fröhlich, F. A systematic approach to identify recycling endocytic cargo depending on the GARP complex. *eLife* **2019**, *8*, No. e42837.
(62) Suda, Y.; Kurokawa, K.; Hirata, R.; Nakano, A. Rab GAP cascade regulates dynamics of Ypt6 in the Golgi traffic. *Proc. Natl. Acad. Sci.* **2013**, *110*, 18976.
(63) Sakane, H.; Yamamoto, T.; Tanaka, K. The Functional Relationship between the Cdc50p-Drs2p Putative Aminophospholipid Translocase and the Arf GAP Gcs1p in Vesicle Formation in the Retrieval Pathway from Yeast Early Endosomes to the TGN. *Cell Structure and Function* **2006**, *31*, 87−108.
(64) Gall, W. E.; Geething, N. C.; Hua, Z.; Ingram, M. F.; Liu, K.; Chen, S. I.; Graham, T. R. Drs2p-Dependent Formation of Exocytic Clathrin-Coated Vesicles In Vivo. *Curr. Biol.* **2002**, *12*, 1623−1627.
(65) Pagani, M. A.; Casamayor, A.; Serrano, R.; Atrian, S.; Ariño, J. Disruption of iron homeostasis in Saccharomyces cerevisiae by high zinc levels: a genome-wide study. *Mol. Microbiol.* **2007**, *65*, 521−537.
(66) Weber, M.; Chernov, K.; Turakainen, H.; Wohlfahrt, G.; Pajunen, M.; Savilahti, H.; Jäntti, J. Mso1p Regulates Membrane Fusion through Interactions with the Putative N-Peptide−binding Area in Sec1p Domain 1. *Mol. Biol. Cell* **2010**, *21*, 1362−1374.
(67) Marash, M.; Gerst, J. E. t-SNARE dephosphorylation promotes SNARE assembly and exocytosis in yeast. *EMBO J.* **2001**, *20*, 411−421.
(68) Saksena, S.; Sun, J.; Chu, T.; Emr, S. D. ESCRTing proteins in the endocytic pathway. *Trends Biochem. Sci.* **2007**, *32*, 561−573.
(69) Jo, W. J.; Loguinov, A.; Chang, M.; Wintz, H.; Nislow, C.; Arkin, A. P.; Giaever, G.; Vulpe, C. D. Identification of Genes Involved in the Toxic Response of Saccharomyces cerevisiae against Iron and Copper Overload by Parallel Analysis of Deletion Mutants. *Toxicol. Sci.* **2008**, *101*, 140−151.
(70) Cotruvo, J. A. The Chemistry of Lanthanides in Biology: Recent Discoveries, Emerging Principles, and Technological Applications. *ACS Cent. Sci.* **2019**, *5*, 1496−1506.
(71) Brayshaw, L. L.; Smith, R. C. G.; Badaoui, M.; Irving, J. A.; Price, S. R. Lanthanides compete with calcium for binding to cadherins and inhibit cadherin-mediated cell adhesion. *Metallomics* **2019**, *11*, 914−924.
(72) Edington, S. C.; Gonzalez, A.; Middendorf, T. R.; Halling, D. B.; Aldrich, R. W.; Baiz, C. R. Coordination to lanthanide ions distorts binding site conformation in calmodulin. *Proc. Natl. Acad. Sci.* **2018**, *115*, E3126.
(73) Kakimoto, M.; Kobayashi, A.; Fukuda, R.; Ono, Y.; Ohta, A.; Yoshimura, E. Genome-Wide Screening of Aluminum Tolerance in Saccharomyces cerevisiae. *BioMetals* **2005**, *18*, 467−474.
(74) Bleackley, M. R.; Young, B. P.; Loewen, C. J. R.; MacGillivray, R. T. A. High density array screening to identify the genetic requirements for transition metal tolerance in Saccharomyces cerevisiae. *Metallomics* **2011**, *3*, 195−205.
(75) Champoux, J. J. DNA Topoisomerases: Structure, Function, and Mechanism. *Annu. Rev. Biochem.* **2001**, *70*, 369−413.
(76) Featherston, E. R.; Issertell, E. J.; Cotruvo, J. A., Jr. Probing Lanmodulin's Lanthanide Recognition via Sensitized Luminescence Yields a Platform for Quantification of Terbium in Acid Mine Drainage. *J. Am. Chem. Soc.* **2021**, *143*, 14287−14299.
(77) Leustek, T.; Murillo, M.; Cervantes, M. Cloning of a cDNA Encoding ATP Sulfurylase from Arabidopsis thaliana by Functional Expression in Saccharomyces cerevisiae. *Plant Physiol.* **1994**, *105*, 897−902.
(78) Murillo, M.; Leustek, T. Adenosine-5′-Triphosphate-Sulfurylase from Arabidopsis thaliana and Escherichia coli Are Functionally Equivalent but Structurally and Kinetically Divergent: Nucleotide Sequence of Two Adenosine-5′-Triphosphate-Sulfurylase cDNAs from Arabidopsis thaliana and Analysis of a Recombinant Enzyme. *Arch. Biochem. Biophys.* **1995**, *323*, 195−204.

https://doi.org/10.1021/acsomega.2c04045
ACS Omega 2022, 7, 34412−34419